

## TURBULENT PENETRATIVE AND RECIRCULATING FLOW IN A COMPARTMENT FIRE

Abdukarim H. Abib and Yogesh Jaluria  
Department of Mechanical and Aerospace Engineering  
Rutgers, The State University of New Jersey  
New Brunswick, New Jersey

### ABSTRACT

A numerical study of a turbulent penetrative and recirculating flow induced by the energy input due to a fire at the bottom boundary in a partially open rectangular enclosure is carried out. The compartment with an opening is connected to a long corridor, which opens into a stably stratified environment. The stable stratification that is of interest is a two-layered temperature stratification and is assumed to be due to fire activity in an adjacent enclosure. In this study, attention is focused on the interaction between the cavity and its surrounding ambient medium through the opening. The influence of the stratification parameter is examined in the turbulent flow regime by considering a range of stratification levels for given opening height and initial interface location.

It is found that, depending on the stratification parameter, the thermal plume that arises above the fire may never reach the ceiling. Small penetration distances occur at large stratification levels. The flow field reveals a multicellular pattern: a strong main convective cell at the bottom and a weak counter cell at the top. The stable thermal stratification can cause a destruction of the turbulence and may thus lead to reduced mixing in the flow. This results in the relaminarization of the flow in the upper region of the cavity and may significantly affect the transport processes in the enclosure and distort the simplistic concept of two homogeneous gas layers, which forms the basis of zone modeling for compartment fires.

### NOMENCLATURE

$A$  aspect ratio,  $A = L/H$   
 $C_{1e}, C_{2e}$  empirical constants in Eq. (7)  
 $C_{3e}$  empirical constant in Eq. (7)  
 $C_{\mu}$  empirical constant in Eq. (8)  
 $\sigma_e, \sigma_k, \sigma_\epsilon$  turbulent Prandtl numbers  
 $g$  magnitude of the gravitational acceleration,  $[m/sec^2]$   
 $Gr$  Grashof number based on the height of the cavity  
 $Gr = g\beta\frac{Q_0}{\kappa}H^3/\nu^2$   
 $H$  height of the compartment,  $[m]$   
 $H_i$  height of the interface,  $[m]$

$H_0$  height of the opening,  $[m]$   
 $K$  dimensionless turbulent kinetic energy  
 $L$  length of the compartment in  $[m]$   
 $L_e$  length of the extended computational domain,  $[m]$   
 $L_f$  size of the fire,  $[m]$   
 $L_i$  length of the doorway soffit,  $[m]$   
 $\dot{m}$  dimensionless mass outflow rate at compartment opening  
 $\overline{Nu_s}$  average Nusselt number over the fire defined in Eq. (18)  
 $Pr$  Prandtl number,  $Pr = \frac{\mu}{\kappa}$   
 $S$  stratification Parameter,  $S = \Delta T_i/\Delta T_q$   
 $Q_0$  Total heat input by the fire per unit width,  $[w/m]$   
 $\dot{q}'''$  heat generation per unit volume,  $[w/m^3]$   
 $t$  dimensionless time  
 $\Delta t$  dimensionless time step  
 $T$  temperature,  $[^\circ K]$   
 $\Delta T_i$  ambient temperature rise,  $[^\circ K]$   
 $\Delta T_q$  characteristic temperature difference,  $\Delta T_q = Q_0/\kappa$ ,  
 $[^\circ K]$   
 $u, v$  dimensionless velocity components in the x and y axes  
 $X$  horizontal coordinate distance from the back wall,  $[m]$   
 $x, y$  dimensionless horizontal and vertical coordinates,  
 $X/H, Y/H$   
 $X_s$  distance between the fire and the back wall,  $[m]$   
 $Y$  vertical coordinate distance from the room floor,  $[m]$   
 $Z_i$  dimensionless height of hot-cold interface

### Greek

$\alpha$  thermal diffusivity,  $[m^2/sec]$   
 $\beta$  coefficient of thermal expansion,  $\beta = \frac{1}{T}$  for perfect gas,  
 $[^\circ K^{-1}]$   
 $\gamma$  dimensionless ambient temperature gradient define in  
Eq.(11)  
 $\delta_p$  dimensionless penetration height of the thermal plume  
 $\epsilon$  dimensionless turbulent kinetic energy dissipation  
 $\varphi$  dimensionless temperature,  $\varphi = \frac{T-T_{\infty,0}}{\Delta T_q} = \Theta +$

$$\frac{T_{\infty,y} - T_{\infty,0}}{\Delta T_q}$$

$\kappa$	coefficient of thermal conductivity, [ $w/m^\circ K$ ]
$\nu$	kinematic viscosity, [ $m^2/sec$ ]
$\nu_e$	effective eddy diffusivity, $(1 + \nu_t/\nu)$
$\nu_t$	turbulent eddy diffusivity, [ $m^2/sec$ ]
$\rho$	density, [ $kg/m^3$ ]
$\Theta$	dimensionless temperature, $\Theta = \frac{T - T_{\infty,y}}{\Delta T_q}$
$\psi$	dimensionless stream function
$\zeta$	dimensionless vorticity

#### Subscripts

$e$	reference to effective value of turbulent eddy diffusivity
$i$	reference to hot-cold interface
$s$	reference to the heat source or fire
$w$	wall value
$\infty, y$	ambient value at a vertical location $y$
$\infty, 0$	ambient value at the lower-layer ( $y = 0$ ) in two-layer system
$\infty, u$	ambient value at the upper-layer in a two-layer system.

## INTRODUCTION

The buoyancy-induced turbulent flow in a partially open cavity with a localized heat source, such as a fire, at the bottom boundary has been studied earlier by Kawagoe (1958), Ku et al. (1976), Emmons (1978), Satoh et al. (1980), Steckler et al. (1982), Markatos et al. (1982), Markatos & Pericleous (1983), and Simcox et al. (1989). In all of these studies, the effects of environmental factors such as the thermal stratification of the ambient medium surrounding the opening or the thermal stratification generated within the cavity did not receive much attention. However, a considerable amount of work has been done over the past three decades on external flows such as plumes and boundary layers in the presence of a stable, thermal ambient stratification. The results have been summarized by Turner (1973), Jaluria (1980), and List (1982). On the other hand, results for cavity or complete enclosure flows with stratification are much less extensive, but include the studies of Walin (1971), Chen et al. (1971), and Torrance (1979). Some work has also been recently done by Abib & Jaluria (1992) considering laminar flows in a partially open enclosure with stably stratified environment.

The flow in an open cavity, such as that due to a fire in a compartment, will interact with its surroundings through the opening. The ambient medium may be thermally stratified due to some earlier fire activity or due to fire in a different location (Cooper et al. 1982). It is well known that, in such natural convection flows, the mean velocity levels are typically smaller and the disturbance levels much larger than those observed in forced flows (Jaluria 1980). This disturbance or turbulence level is of interest, because it enhances mixing and thus promotes transport of both momentum and energy. As a result, a well-mixed region of essentially uniform temperature is generated in the compartment fire. The stratification level is also of particular importance, because its influence is felt in two ways (McCaffrey & Quintiere 1977). At first, in an enclosure fire, it affects the location of the interface between the hot combustion products and the cold inflow at bottom (hot-cold interface) by inhibiting the rise of fire or thermal plume above the heat source. The knowl-

edge of the location of the hot-cold interface is, therefore, very crucial to the detection and control of a fire. Secondly, when the thermal stratification is stable, it results in a decay of the turbulence and, hence, leads to a re-laminarization of the flow (see the review by Quintiere 1984). This may then alter the transport processes and distort the simplistic concept of two homogeneous gas layers, which form the basis of the zone modeling analysis of room fires. The primary objective of the present work is to study the influence of the ambient temperature stratification in turbulent regime.

## MATHEMATICAL FORMULATION

### The Problem

A numerical study of the turbulent recirculating flow due to energy input by a fire at the bottom boundary of a partially open rectangular cavity of height  $H$  and aspect ratio (height to length)  $A$  of 2, typical of room-size enclosures, is carried out. The partially open enclosure (or compartment) is in communication with a long corridor through the opening (Fig. 1). The corridor surrounding the opening is considered to be stably stratified due to the thermal energy input from various sources such as a fire at the far end of the corridor or an adjacent room. The stratification is maintained essentially unchanged over long periods of time as long as there is an energy input. In modeling the environmental conditions, a two-layer temperature stratification which is usually encountered in room fires (see Cooper et al. 1982) is appropriate. The compartment and the surrounding environment are considered to be initially stratified. After the

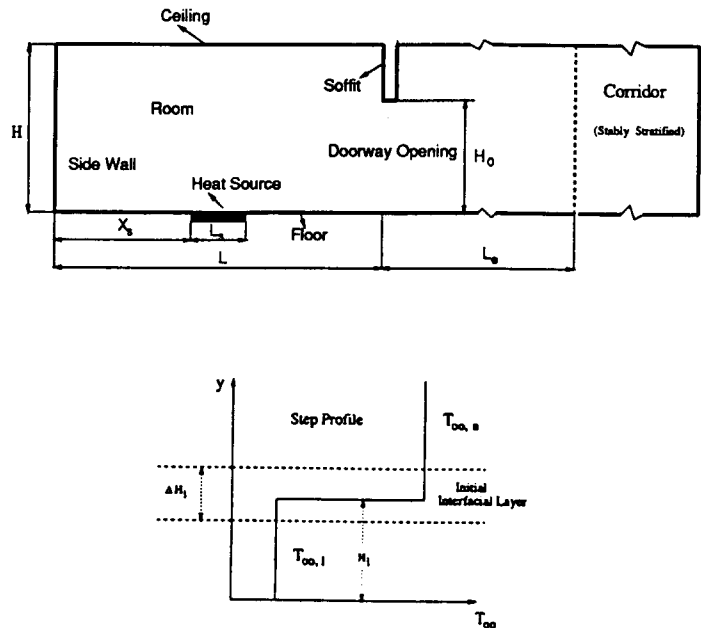


Figure 1: Room and corridor system with a step ambient temperature stratification.

onset of the fire, the environment at the far end of the corridor is assumed to remain stably stratified.

The phenomenological aspects of fire spread in a room following ignition are illustrated in Fig. 2. The gases in the room may be characterized in terms of upper and lower zones, separated by a stably stratified interface and affected by shear-induced mixing near the opening. The fire plume in the center thus penetrates this stratified medium.

For the present study, following other earlier work, the fire is replaced by a localized heat source with a constant heat input per unit width,  $Q_0$ . Work has been done on the combined radiative and convective transport in gases enclosed in a room with fire (Larson & Viskanta 1976, Yang & Lloyd 1985, and Fusegi & Farouk 1989, among others). But in the present study, the role of radiation in the gases is ignored and the focus is on convective flow and transport, since interest lies in regions far from the fire. However, the radiative loss from the fire to the walls is accounted for by using a corrected heat input to the gases. This is usually a reasonable approximation for small scale fires ( $Gr < 10^{13}$ ). Also, convective mechanisms dominate far from the combustion zone.

Adiabatic boundary conditions are considered at the side walls, the floor and the ceiling, assuming that these have heated up and are well-insulated. Only a single doorway opening is examined to represent typical room fires. Also, higher stratification levels are associated with this case.

For a stratified ambient medium, the influence of the stratification parameter is examined in the turbulent flow regime by considering a range of stratification levels for a given opening height (say  $H_0 = 0.8H$ ) and initial interface location (say

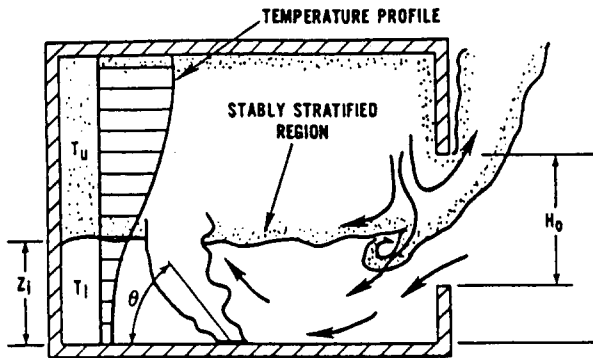


Figure 2: The phenomenological aspect of fire spread in an enclosure.

$H_i = 0.5H$ ). The effort is mainly directed at determining the heat transfer rate, mass flow rate, the penetration distance of the thermal plume rising above the energy source, and the turbulence and stratification levels that are generated within the cavity, in order to characterize the resulting penetrative and recirculating flow.

### Governing Equations

Using  $H$ ,  $\Delta T_q$ , and  $H/\sqrt{g\beta\Delta T_q H}$  as reference length, temperature, and time scales, respectively, the governing equations, in dimensionless form, expressing conservation of mass, momentum, energy, and the turbulent kinetic energy and its dissipation, for incompressible Boussinesq fluid, can be written as:

$$u = \frac{\partial \psi}{\partial y}; \quad v = -\frac{\partial \psi}{\partial x} \quad (1)$$

$$\frac{\partial^2 \psi}{\partial x^2} + \frac{\partial^2 \psi}{\partial y^2} = -\zeta \quad (2)$$

$$\begin{aligned} \frac{\partial \zeta}{\partial t} + \frac{\partial(u\zeta)}{\partial x} + \frac{\partial(v\zeta)}{\partial y} &= \frac{1}{\sqrt{Gr}} \left\{ \frac{\partial}{\partial x} \left( \frac{\partial(\nu_e \zeta)}{\partial x} \right) \right. \\ &\quad \left. + \frac{\partial}{\partial y} \left( \frac{\partial(\nu_e \zeta)}{\partial y} \right) \right\} + S_\zeta \end{aligned} \quad (3)$$

$$\begin{aligned} \frac{\partial \Theta}{\partial t} + \frac{\partial(u\Theta)}{\partial x} + \frac{\partial(v\Theta)}{\partial y} + v\gamma &= \frac{1}{Pr\sqrt{Gr}} \left\{ \frac{\partial}{\partial x} (\nu_{e,\theta} \frac{\partial \Theta}{\partial x}) \right. \\ &\quad \left. + \frac{\partial}{\partial y} (\nu_{e,\theta} \frac{\partial \Theta}{\partial y}) \right\} \\ &\quad + \frac{1}{Pr\sqrt{Gr}} \left\{ \dot{q}''' + \frac{d^2 \Theta_{\infty, v}}{dy^2} \right\}. \end{aligned} \quad (4)$$

$$\begin{aligned} \frac{\partial K}{\partial t} + \frac{\partial(uK)}{\partial x} + \frac{\partial(vK)}{\partial y} &= \frac{1}{Pr\sqrt{Gr}} \left\{ \frac{\partial}{\partial x} (\nu_{e,k} \frac{\partial K}{\partial x}) \right. \\ &\quad \left. + \frac{\partial}{\partial y} (\nu_{e,k} \frac{\partial K}{\partial y}) \right\} + P + G - \epsilon \end{aligned} \quad (5)$$

$$\begin{aligned} \frac{\partial \epsilon}{\partial t} + \frac{\partial(u\epsilon)}{\partial x} + \frac{\partial(v\epsilon)}{\partial y} &= \frac{1}{Pr\sqrt{Gr}} \left\{ \frac{\partial}{\partial x} (\nu_{e,\epsilon} \frac{\partial \epsilon}{\partial x}) + \frac{\partial}{\partial y} (\nu_{e,\epsilon} \frac{\partial \epsilon}{\partial y}) \right\} \\ &\quad + \frac{\epsilon}{K} \{ C_{1\epsilon} f_1 (P + C_{3\epsilon} G) \\ &\quad - C_{2\epsilon} f_2 \epsilon \} \end{aligned} \quad (6)$$

where  $S_\zeta$  is the source terms for the mean vorticity equation given by

$$S_\zeta = \frac{\partial \Theta}{\partial x} + \frac{1}{\sqrt{Gr}} \left\{ 2 \left( \frac{\partial u}{\partial y} \right) \frac{\partial^2 \nu_e}{\partial x^2} - 2 \left( \frac{\partial v}{\partial x} \right) \frac{\partial^2 \nu_e}{\partial y^2} + 4 \left( \frac{\partial v}{\partial y} \right) \frac{\partial^2 \nu_e}{\partial y \partial x} \right\}$$

and  $G$  and  $P$  are buoyancy and shear production of the turbulent kinetic energy defined as

$$\begin{aligned} G &= -\frac{1}{\sqrt{Gr}} \frac{\nu_t^*}{\sigma_t} \frac{\partial \Theta}{\partial y} \\ P &= \frac{\nu_t^*}{\sqrt{Gr}} \left\{ \left( \frac{\partial u}{\partial y} + \frac{\partial v}{\partial x} \right)^2 + 2 \left( \frac{\partial u}{\partial x} \right)^2 + 2 \left( \frac{\partial v}{\partial y} \right)^2 \right\} \end{aligned} \quad (7)$$

with

$$\nu_t^* = \frac{\nu_t}{\nu} = \sqrt{Gr} f_\mu C_\mu \frac{K^2}{\epsilon} \quad (8)$$

Here  $\nu_e$ ,  $\nu_{e,\theta}$ ,  $\nu_{e,k}$ , and  $\nu_{e,\epsilon}$  are effective turbulent diffusivities defined as

$$\nu_e = 1 + \nu_t^*; \quad \nu_{e,\theta} = 1 + \frac{Pr\nu_t^*}{\sigma_t}; \quad \nu_{e,k} = 1 + \frac{\nu_t^*}{\sigma_k}; \quad \nu_{e,\epsilon} = 1 + \frac{\nu_t^*}{\sigma_\epsilon}$$

The damping wall functions  $f_1$ ,  $f_2$ , and  $f_\mu$  for modified low-Reynolds ( $k-\epsilon$ )-model of Lam Bremhorst (see Davidson 1990), here-after denoted as MLB, are:

$$\begin{aligned} f_1 &= 1 + \left(\frac{0.14}{f_\mu}\right)^3 \\ f_2 &= [1 - 0.27 \exp(-Re_t^2)][1 - \exp(-Re_n)] \\ f_\mu &= \exp\left\{-\frac{3.4}{(1 + Re_t/50)^2}\right\} \quad Re_t = \frac{K^2}{\nu \epsilon} \quad Re_n = \frac{\sqrt{K}}{\nu} \end{aligned} \quad (9)$$

where  $n$  is the normal distance from the nearest fixed wall.

The coefficients  $C_\mu$ ,  $C_{1\epsilon}$ ,  $C_{2\epsilon}$ ,  $C_{3\epsilon}$ ,  $\sigma_t$ ,  $\sigma_k$ , and  $\sigma_\epsilon$  are empirical constants given in Table 1. These constants are recommended by Launder & Spalding (1974), except for the constant  $C_{3\epsilon}$  in the buoyancy term of the  $\epsilon$ -equation, which is suggested by Rodi (1980) to be close to 1 in vertical boundary layers and close to 0 in horizontal layers. For the present work  $C_{3\epsilon}$  was adopted from Fraikin et al. (1980) as  $C_{3\epsilon} = 0.7/C_{1\epsilon}$ . All the

Table 1: Empirical constants for ( $K-\epsilon$ )-model recommended by Launder & Spalding (1974).

$C_\mu$	$C_{1\epsilon}$	$C_{2\epsilon}$	$C_{3\epsilon}$	$\sigma_\theta$	$\sigma_k$	$\sigma_\epsilon$
0.09	1.44	1.92	0.7	0.9	1.0	1.3

symbols are defined in the nomenclature. When considering the two-layer ambient temperature, a sharp interface is physically not reasonable and the temperature jump at the interface is approximated by a gradual rise, using the following expression

$$T_{\infty,y} = 0.5 \Delta T_i \left\{ 1 + \tanh\left[b\left(\frac{Y}{H} - \frac{H_i}{H}\right)\right] \right\} \quad (10)$$

where  $\Delta T_i$  is the temperature jump at the interface,  $b = 2/\Delta H_i$  is the compression ratio,  $H_i$  is the height of the interface and  $\Delta H_i$  is the height of the interfacial layer. The dimensionless ambient temperature gradient  $\gamma$  for the two-layer ambient temperature profile is given by

$$\gamma = \frac{H}{\Delta T_q} \frac{dT_{\infty,y}}{dY} = 0.5 b \frac{\Delta T_i}{\Delta T_q} \operatorname{sech}^2\left[b\left(\frac{Y}{H} - H_i\right)\right]. \quad (11)$$

The ratio  $S = \Delta T_i/\Delta T_q$  that appears in the expression of the ambient temperature gradient  $\gamma$  is called the stratification parameter. The stratification parameter  $S$  can also be considered as the dimensionless temperature rise at the interface. Since the dimensionless temperature  $\Theta$  is defined relative to the ambient temperature  $T_{\infty,y}$  an extra term  $v\gamma$  appears in the energy equation (Eq. (4)). This term describes the vertical convection in a stratified medium. In an isothermal ambient case,  $T_{\infty,y}$  is constant and the extra term becomes zero.

The governing equations introduce three dimensionless parameters: the Grashof number  $Gr$ , the Prandtl number  $Pr$ , and the stratification parameter  $S$ . Since the fluid considered is air the Prandtl number  $Pr$  is set to a value of 0.72. The size of the fire  $L_s$  is set equal to  $0.2H$  and the location is taken as  $X_s = 0.9H$ .

### Initial and Boundary Conditions

The initial and boundary conditions for the governing equations (1) - (6) are specified as

- Initial condition at  $t < 0$ :  
isothermal or stably stratified room and environment. Laminar  $u$ -,  $v$ -,  $\psi$ -,  $\zeta$ - profiles specified,  $\Theta = 0$ , and non-zero perturbations in  $K$  and  $\epsilon$ , typically:

$$K = 10^{-6}, \quad \nu_t^* = \frac{\nu_t}{\nu} = 10, \quad \epsilon = \sqrt{Gr} C_\mu \frac{K^2}{\nu_t^*} \quad (12)$$

- Boundary conditions at  $t \geq 0$ :

1. Bottom boundary (floor) at  $y = 0$ :

$$u = v = \psi = K = \frac{\partial \epsilon}{\partial y} = 0, \quad \zeta = \zeta_w, \quad 0 \leq x \leq x_{max}$$

$$\frac{\partial \Theta}{\partial y} = \begin{cases} 0 & 0 \leq x \leq x_s \\ \dot{q}_o'' = \frac{1}{l_i} & x_s \leq x \leq x_s + l_i \\ 0 & x_s + l_i \leq x \leq x_{max} \end{cases}$$

2. Ceiling at  $y = 1$  and doorway soffit at  $y = h_0$ :

$$u = v = \psi = K = \frac{\partial \epsilon}{\partial y} = \frac{\partial \Theta}{\partial y} = 0, \\ \zeta = \zeta_w, \quad 0 \leq x \leq x_{max}$$

3. Left side wall or back wall at  $x = 0$ :

$$u = v = \psi = K = \frac{\partial \epsilon}{\partial x} = \frac{\partial \Theta}{\partial x} = 0, \\ \zeta = \zeta_w, \quad 0 \leq y \leq 1 \quad (13)$$

4. Door soffit walls at  $x = A$  and  $x = A + l_i$ :

$$u = v = \psi = K = \frac{\partial \epsilon}{\partial x} = 0, \quad \zeta = \zeta_w \\ \frac{\partial \Theta}{\partial x} = 0, \quad h_0 \leq y \leq 1$$

5. Right far-field boundary at  $x = x_{max}$ :

$$v = \frac{\partial u}{\partial x} = \frac{\partial \psi}{\partial x} = \frac{\partial \zeta}{\partial x} = \frac{\partial K}{\partial x} = \frac{\partial \epsilon}{\partial x} = 0, \quad 0 \leq y \leq 1$$

$$\begin{cases} \Theta = 0 & \text{if } u \leq 0 & (\text{inflow}) \\ \frac{\partial \Theta}{\partial x} = 0 & \text{if } u > 0 & (\text{outflow}) \end{cases}$$

For the wall vorticity  $\zeta_w$ , a first-order form first given by Thom (1928, cited in Roache 1972) is used

$$\zeta_w = -2 \frac{\psi_{w+1} - \psi_w}{\Delta n^2} + O(\Delta n) \quad (14)$$

where  $n$  is the direction normal to wall. This first-order form is the safest form to use and often gives results essentially equal to the higher-order forms (Roache, 1972).

### NUMERICAL SOLUTION

The statistically averaged equations governing the mean-flow quantities are given in Eqs. (1) - (6). Despite the time-averaging, the unsteady terms are kept in the formulation of the governing equations to account for unsteadiness in the transport processes. In other words, according to Rodi (1987), the averaging is carried out over-all turbulent motions, i.e. over a time period that is larger than the time scale of turbulence. However, the averaging time is smaller than the time scale of non-turbulent mean

motion. In an enclosure, the latter is basically determined by the time scale of the internal gravity waves. Since we are only interested in the large-time behavior of Reynolds-averaged equations, we use the results to check if the unsteadiness has died out and if a steady state solution is reached.

The details of the numerical scheme used are given by Abib (1992). The governing equations are discretized with the control-volume based finite-difference method. The advection and diffusion terms are discretized with the power-law scheme (Patankar, 1980). Due to the non-linearities in the advection terms and in the boundary conditions and due to the decoupled nature of numerically solving the transport equations, it is necessary to use an iterative method for the solution of the system of discretized equations. The temporal discretization is executed implicitly. The solution for  $\Theta$ ,  $\zeta$ ,  $\psi$ ,  $K$ , and  $\epsilon$  is obtained by an iterative procedure at each time step. The iterative method is a double loop in which the inner loop is a line by line method, in which tridiagonal matrix is inverted in each sweep direction, for the variables  $\Theta$ ,  $\zeta$ ,  $K$ , and  $\epsilon$ , and the SOR method is employed for  $\psi$ . Because of the non-linearity, it was necessary to under-relax both the interior field and boundary points of the discretized equations.

The existence of a thin boundary layer near the walls requires that a non-uniform grid be used that gives a strong grid refinement near the walls. A hyperbolic grid distribution was used, defined as

$$\frac{X_i}{H} = \frac{1}{2} \left\{ 1 + \frac{\tanh[\alpha_1(i/i_{max} - \frac{1}{2})]}{\tanh(\alpha_1/2)} \right\} \quad i = 0, 1, 2, \dots, i_{max} \quad (15)$$

$$\frac{Y_i}{H} = \frac{1}{2} \left\{ 1 + \frac{\tanh[\alpha_2(i/i_{max} - \frac{1}{2})]}{\tanh(\alpha_2/2)} \right\} \quad i = 0, 1, 2, \dots, i_{max} \quad (16)$$

where  $\alpha_1$  is given by  $\alpha_2 = \alpha_1 / \sinh(\alpha_1)$ . In all the calculations,  $\alpha_2$  is taken as  $1.5 \times 10^{-3}$  which gives  $\alpha_1 = 6.811$ , to ensure that at least 8 to 10 points lie between the wall and the location of maximum velocity in the boundary layer. In the y-direction, extra grid points are added at the location of the interface of a step ambient temperature profile in order to resolve sharp gradients. Also, in the x-direction, extra points (10 points) are added near the location of the heat source. In order to ensure numerical accuracy of the results the computational mesh is refined from  $50 \times 50$  (with  $30 \times 30$  points inside the room) to  $100 \times 100$  (with  $60 \times 60$  inside the room).

Using the analogy of buoyancy-driven flows in a cavity with differentially heated side walls (see Gills 1966, Patterson & Imberger 1980, and Henkes 1990), the time evolution in the open cavity at large  $Gr$  is dominated by two time scales:

$$t_1 = \frac{A^2 H^2}{\nu} (GrPr)^{-1/4} \quad \text{and} \quad t_2 = \frac{H^2}{\nu} (GrPr)^{-1/2}. \quad (17)$$

The diffusion time scale  $t_0 = \frac{H^2}{\nu} (GrPr)^0$  is the dominant time scale at small  $Gr$ , but is of minor importance at large  $Gr$ . The time scale  $t_1$  is larger than  $t_2$  and determines the needed time to reach the steady state. The time scale  $t_2$  is the Brunt-Vaisala time scale and determines the maximum time step that still gives a stable numerical solution. This time step limitation has also been reported by Thompson et al. (1987), Henkes (1990), and Davidson (1990) from their study of buoyancy-driven turbulent flow in a rectangular cavity. The required number of time steps

is estimated as  $t_{max} = \frac{t_1}{t_2} = A^2 (GrPr)^{1/4}$ . For all cases, a time step  $\Delta t = \frac{1}{10}$  or  $\frac{1}{5}$  is used to ensure a stable numerical solution.

Initially, the compartment and the surrounding environment is considered to be stably stratified (i.e.  $\Theta = 0$ ). After the onset of fire in the compartment, the environment at the far end ( $x = x_{max}$ ) is assumed to remain stratified. The initial conditions for Eqs. (5) and (6) can be obtained from non-zero perturbations in  $K$  and  $\epsilon$ . Typical values of  $K_0$  is  $10^{-6}$ ,  $\nu_t^*$  is in the range from 2 to 10 and  $\epsilon_0$  is evaluated as  $Gr^{1/2} C_\mu K_0^2 / (\nu_t^*)_0$ . The values of  $K_0$  and  $(\nu_t^*)_0$  have been varied and have a negligible effect on the computed results.

## RESULTS AND DISCUSSION

The influence of ambient medium stratification in a partially open cavity has been addressed by Abib & Jaluria (1992), considering small values of  $Gr$  so that the resulting buoyancy-induced flow remains laminar. We are now interested in the turbulent regime which is of much greater significance for room fires, and consider a partially open cavity with a doorway opening of height  $H_0 = 0.8H$ , with adiabatic walls and with a fire located at the middle of the bottom boundary ( $X_s = 0.9H$ ). A step ambient temperature distribution is considered. The results reported here refer to  $Gr = 2 \times 10^{10}$  and the ambient temperature stratification parameter  $S$  is varied from 0.005 to 0.05. These values are selected so that both weak and strong thermal stratification can be simulated.

Steady state solution is sought, as before, by numerically solving the initial-value problem. For values of  $Gr \geq 2 \times 10^8$ , the achievement of a true steady state is made difficult by the presence of the internal gravity waves, in particular, when the medium is stratified. This problem was discussed in detail by Abib & Jaluria (1992) for  $Gr = 2 \times 10^7$  and  $Gr = 2 \times 10^8$ . This discussion is also valid for  $Gr = 2 \times 10^{10}$ . The only difference is that the amplitude is slightly larger due to the higher value of  $Gr$ . For instance, at  $Gr = 2 \times 10^{10}$ , oscillations are shown in Fig. 3 for the average Nusselt number  $\overline{Nu_s}$ , define as

$$\overline{Nu_s} = \frac{1}{l_s^2} \int_0^{l_s} \frac{1}{\Theta_s} dx. \quad (18)$$

and the eddy diffusivity  $(\nu_t/\nu)_1$  at a point in the cavity with coordinates  $x=0.138$ ,  $y=0.158$ . The stream function  $\psi_c$  and the eddy diffusivity  $(\nu_t/\nu)_c$  at the center of the cavity ( $x=1.0$ ,  $y=0.5$ ) are also shown in Fig. 4. The amplitude of the stream function oscillations are less than 3-5% of the mean, while those of the temperature are slightly higher (5-10% of the mean). For the average quantities such as the heat transfer rate over the fire  $\overline{Nu_s}$ , and the mass outflow rate at compartment opening  $\dot{m}\sqrt{Gr}$ , the fluctuations are even less, being 0.2% for the heat transfer rate and 2.5% for the mass flow rate.

## Flow and Thermal Field

The computed steady state flow and thermal fields are shown in Fig. 5 for  $S = 0.005$ . The top graph (a) shows the isotherms<sup>1</sup> and the bottom graph (b) shows the streamlines<sup>2</sup>. The figure shows that the thermal plume, which flows along the back wall,

<sup>1</sup>Temperature contours are scaled by a factor of 100 in order to plot legible labels on the plots.

<sup>2</sup>stream function is scaled by a factor of 1000.

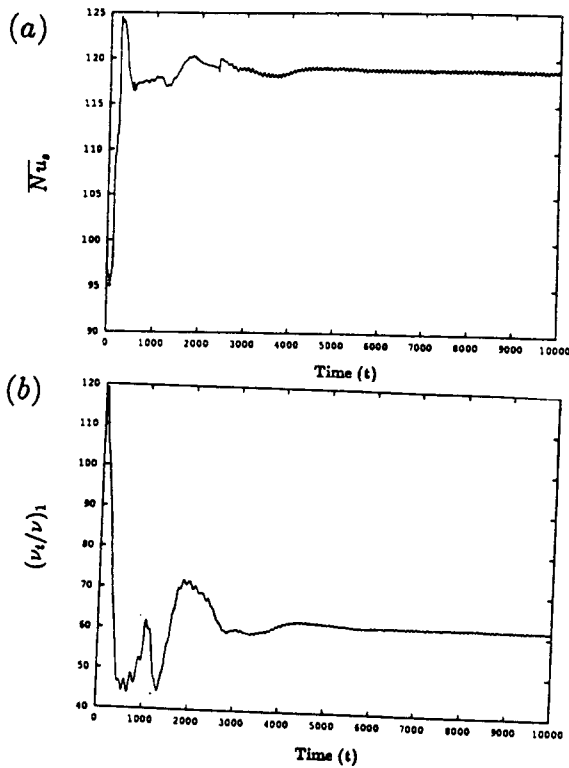


Figure 3: (a) The average Nusselt number at the fire  $\overline{Nu}_a$ , and (b) the turbulent eddy diffusivity  $(\frac{u_i}{v})_1$  at a location ( $x = 0.036$ ,  $y = 0.5$ ) as functions of time in a two-layer stratified ambient with  $S = 0.01$ ,  $Gr = 2 \times 10^{10}$ , and  $H_0 = 0.8H$ .

reaches the ceiling because the thermal stratification of the ambient medium is weak. As the stratification parameter  $S$  is increased to say a value of  $S = 0.01$  (results shown in Fig. 6), the wall plume is unable to reach the ceiling. Two cells are formed, a strong main cell and a weak counter cell. The largest velocities are found in the main convective cell. The flow pattern is similar to that described by Abib & Jaluria (1992), but much more vigorous because of the higher value of  $Gr$ . There is also more mixing in the cavity due to the turbulence which enhances it and, hence, leads to the establishment of isothermal layers at the bottom (lower-layer) and the top (the upper-layer). In the case of an isothermal ambient medium ( $S = 0$ ), the computed steady state flow field agrees qualitatively with fire work (see Abib 1992 for further detail).

### The Mean Velocity and Temperature

The vertical distribution of the temperature  $\varphi$ , at  $Gr = 2 \times 10^{10}$ , for various ambient temperature stratification levels, is shown in Fig. 7. Like the laminar case presented by Abib & Jaluria (1992), the horizontal temperature gradients are small except near the fire and the back wall. Three distinct regions can be identified for the vertical temperature profiles. These are:

- The lower layer which is at an essentially uniform temperature or is slightly stratified, except in the vicinity of the fire and the back wall.
- The intermediate stratified layer. This linearly stratified layer is generated as a consequence of the interaction be-

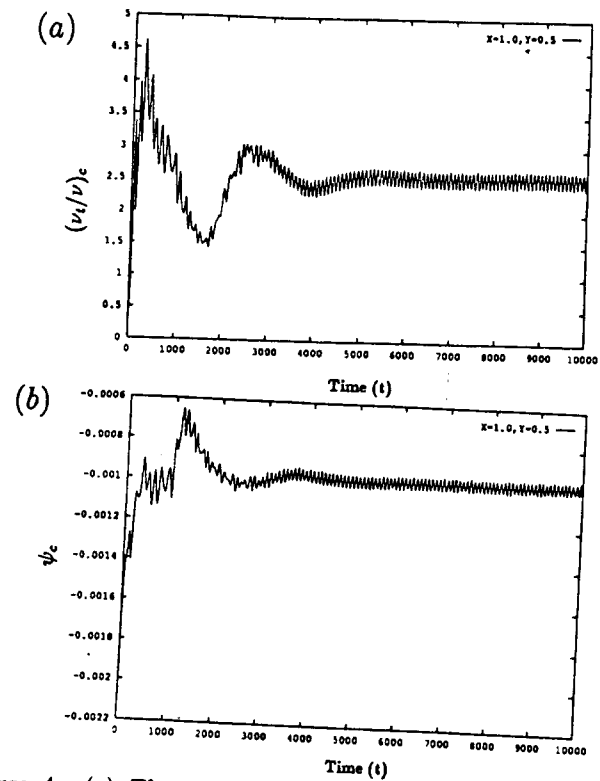


Figure 4: (a) The turbulent eddy diffusivity  $(\frac{u_i}{v})_c$  and (b) the mean stream function  $\psi_c$  at the center of the enclosure as functions of time in a two-layer stratified ambient with  $S = 0.01$ ,  $Gr = 2 \times 10^{10}$ , and  $H_0 = 0.8H$ .

tween the enclosure and the ambient medium.

- The upper layer which is at a uniform temperature. The temperature level in this region is close to or lower than that of the ambient medium at the same height.

The location of the intermediate stratified layer is very hard to define since it varies horizontally. From a visual inspection of the temperature profiles, it is seen that the average height of the intermediate layer is 0.175. The slope  $\gamma$  of the stratified intermediate layer may be considered as a measure of the stratification level. It is observed that the stratification level increases slightly as the stratification parameter of the ambient medium is increased (see Table 2). The generation of the intermediate stratified layer is due to the fact that the rise of fire plume is inhibited by the presence of the stable temperature gradient in the cavity. The plume is confined to a certain height above the interface (the penetration distance) which is below the ceiling (see Table 2). The plume causes a recirculation within the upper and lower layers. As the result of the stirring and mixing, between the cooler layer with fluid from the warmer upper layer, a linearly stratified intermediate layer is generated.

The vertical distributions of the horizontal component of the velocity  $u$ , at  $Gr = 2 \times 10^{10}$ , for various ambient temperature stratification levels  $S$  are shown in Fig. 8. The  $u$ -velocity profiles show a strong convective main cell and a weak counter cell above it in all the cases where  $S \leq 0$ . In the main cell, there is inflow at the bottom and outflow at the top part of the cell. The influence of the ambient stratification parameters is more pronounced in the top part of the main cell, as the outflow is increasingly retarded as  $S$  is increased. This is, of course, due

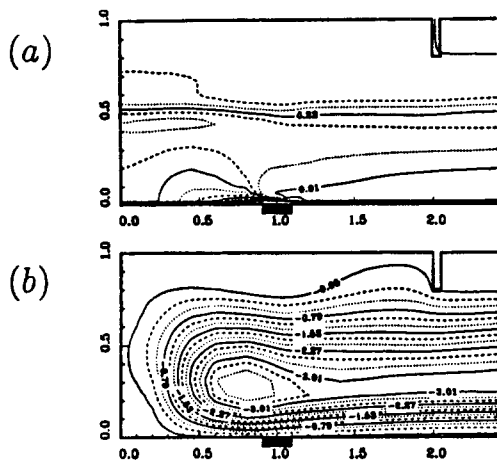


Figure 5: Steady state turbulent flow and thermal field, at  $Gr = 2 \times 10^{10}$ , for a partially open cavity in a two-layer stratified ambient with  $S = 0.005$ . The opening height is  $H_0 = 0.8H$ , wall boundaries are adiabatic, and the fire is located at the middle of the bottom boundary. (a) Isotherms and (b) streamlines.

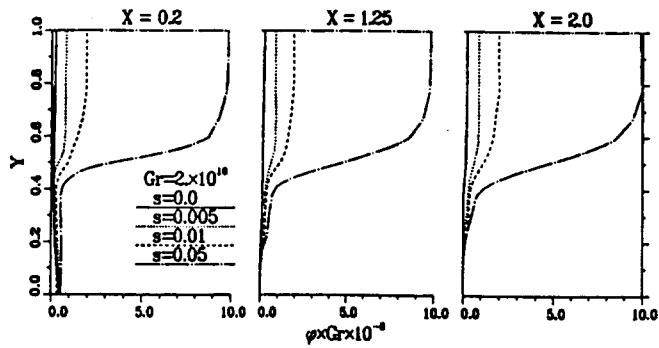


Figure 7: Vertical profiles of the mean temperature  $\phi$ , at  $Gr = 2 \times 10^{10}$ , for a partially open cavity in two-layer stratified ambient with various values of the stratification parameter  $S$ .

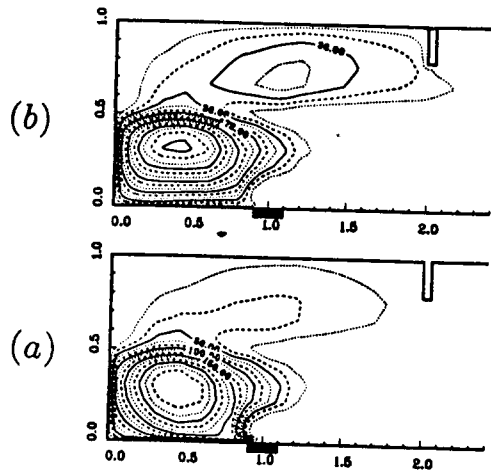


Figure 9: Contour lines of (a) the turbulent kinetic energy  $k$  and (b) the turbulent eddy diffusivity  $\nu_t/\nu$ , at  $Gr = 2 \times 10^{10}$ , for a partially open cavity in a two-layer stratified ambient with  $S = 0.005$ . The opening height is  $H_0 = 0.8H$ , wall boundaries are adiabatic, and the fire is located at the middle of the bottom boundary.

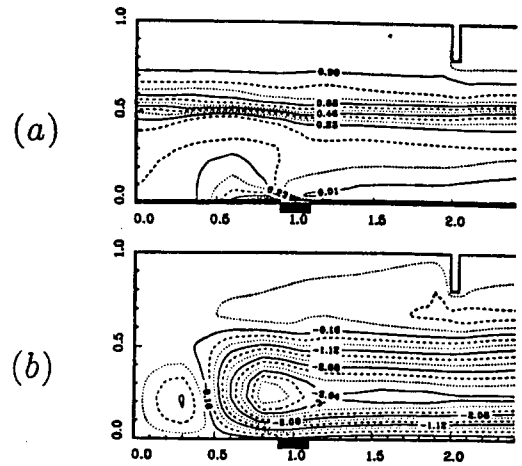


Figure 6: Steady state turbulent flow and thermal field, at  $Gr = 2 \times 10^{10}$ , for a partially open cavity in a two-layer stratified ambient with  $S = 0.01$ . The opening height is  $H_0 = 0.8H$ , wall boundaries are adiabatic, and the fire is located at the middle of the bottom boundary. (a) Isotherms and (b) streamlines.

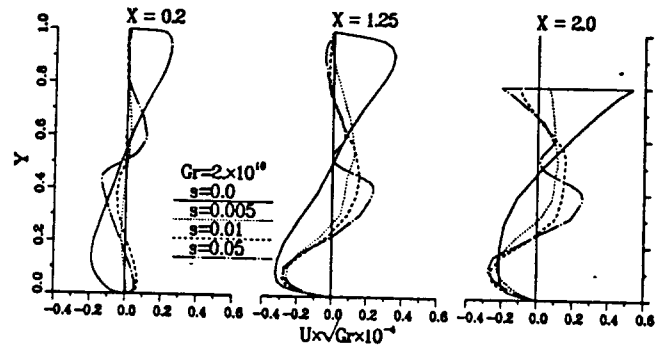


Figure 8: Horizontal component of the mean velocity  $u$  as function of the vertical distance  $y$ , at  $Gr = 2 \times 10^{10}$ , for a partially open cavity in two-layer stratified ambient with various values of the stratification parameter  $S$ .

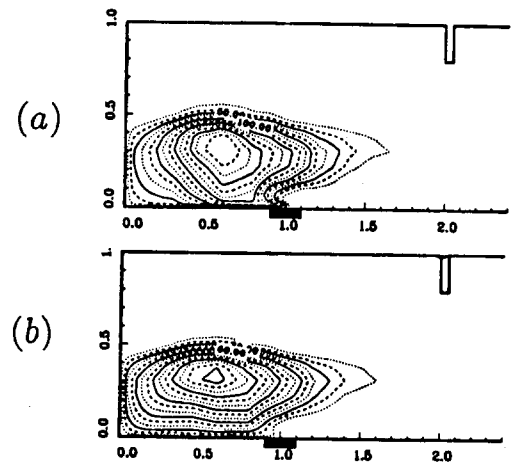


Figure 10: Contour lines of (a) the turbulent kinetic energy  $k$  and (b) the turbulent eddy diffusivity  $\nu_t/\nu$ , at  $Gr = 2 \times 10^{10}$ , for a partially open cavity in a two-layer stratified ambient with  $S = 0.01$ . The opening height is  $H_0 = 0.8H$ , wall boundaries are adiabatic, and the fire is located at the middle of the bottom boundary.

Table 2: The penetration distance  $\delta p$ , the height of the hot-cold interface  $Z_i$ , the stratification level  $\gamma$ , and mass outflow rate  $\dot{m}Gr^{1/2}$  room with an opening, with  $H_0 = 0.8H$  and  $Gr = 2 \times 10^{10}$  for a two-layer stratified environment.

	$S$		
	0.005	0.01	0.05
$\delta p$	0.4	0.425	0.425
$Z_i$	0.3	0.23	0.21
$\gamma$	2.5	2.6	3.0
$\dot{m}\sqrt{Gr}$	$3.575 \times 10^{-3}$	$3.302 \times 10^{-3}$	$3.06 \times 10^{-3}$

to reduction in the local buoyancy caused by the increase in the ambient temperature with height. The mass outflow rate increases with  $Gr$ , for a given doorway opening, because of the larger energy input. However, it decreases with an increase in the ambient stratification (see Table 2) because stratification causes a reduction in the buoyancy level, resulting in a less vigorous flow. In isothermal ambient medium case, the computed mass outflow rate is in a fairly good agreement with results reported in fire literature (see Abib 1992).

### The Turbulent Quantities

As for the turbulent quantities, contour plots of the turbulent kinetic energy<sup>3</sup>  $K$  and the eddy diffusivity  $\nu_t/\nu$  are shown in Figs. 9 and 10, for  $S = 0.005$  and  $S = 0.01$ , respectively. The top graph (a) refers to the kinetic energy, while in the bottom graph (b) refers to the eddy diffusivity.

In the case of a weak ambient stratification (say, for instance,  $S = 0.005$ ) the fire plume is able to penetrate into the upper layer. Turbulence is generated in the region between the fire and the back wall (in the attachment area of the wall plume). From there, it is convected to the upper layer. When the ambient stratification is strong (say  $S \geq 0.01$ ) the plume rise is inhibited by the stable gradient. Turbulence is confined in the left corner between the fire and the back wall where it is generated since the stable gradient will destroy the turbulence. A similar behavior of the turbulence confinement is obtained in the isothermal ambient medium case, but with a smaller opening height (say  $H_0 = 0.3H$ ). This interesting case is discussed in greater detail by Abib (1992).

### Relevance to Zone Modeling Analysis of Room Fires

Zone models have been extensively used to predict the growth of fire in a room by determining the average temperature levels and the flow rates, using turbulent plume analysis and Bernoulli's equation for flow through the doorway opening. The room is divided into distinct homogeneous layers. Each layer is assumed to be at uniform conditions, while different layers are at different conditions (see review by Quintiere 1977). The accuracy of zone models to predict conditions in a room fire depends on the accurate determination of flow rates, energy transport and mixing

<sup>3</sup>Turbulent kinetic energy  $K$  is scaled by a factor of  $10^6$  in order to plot legible contour labels on the plots.

across the interface. However, the suppression of turbulence in the upper part of the room fire by buoyancy and the subsequent re-laminarization of the flow, and the failure of the fire plume to penetrate into the upper layer of the room due to the stable thermal stratification of the environment, may significantly alter the transport processes. These aspects have not yet been included in such models for fire growth studies (Quintiere 1984).

This study addresses the influence of stratification and quantifies it in terms of penetration distance of the fire plume  $\delta p$  and the height of the hot-cold interface  $Z_i$  for a given heat input. In order that this work be useful for zone modeling, correlations for  $\delta p$  and  $Z_i$  as function of Grashof number, opening height and initial stratification are needed. We also need some experimental data and observations of these flow circumstances to compare with numerical results.

### CONCLUSIONS

A study of turbulent penetrative convection, in a compartment fire was carried out. The fire is simulated by a small localized energy source at the bottom boundary. A compartment with a doorway opening is connected to a long corridor which opens into a two-layer stably, thermally stratified ambient medium. The study mainly focuses on the interaction between the compartment and the environment factors such as temperature stratification of the ambient medium at high  $Gr$ .

The results obtained agree qualitatively with fire work. In the range of the stratification parameter  $S$  examined, it was found that for large values of  $S$  the fire plume does not reach the ceiling. The flow reveals a multi-cellular pattern consisting of a strong main cell at the bottom part of the room and a weak counter cell at the top. The penetrative flow takes place in the form of horizontal motion in the upper part of the main cell.

Because of the stable thermal stratification, the rise of the fire plume is inhibited and the hot-cold interface is lowered and, furthermore, the turbulence is suppressed and results in the re-laminarization of the flow in the upper part of room. It, thus, alters the transport processes, leading to reduced mixing in the flow. This may then require changes in the simplistic concept of two homogeneous gas layers which forms the basis of zone modeling analysis of room fires.

### ACKNOWLEDGMENTS

The authors acknowledge the partial support provided by the Building and Fire Research Laboratory, National Institute of Standards and Technology, under Grant No. 60NANB1D1171 for this work.

### REFERENCES

- Abib, A.H., 1992, "Penetrative and Recirculating Flows in Enclosures with Openings", *Ph.D. Thesis*, Rutgers University, New Brunswick, NJ.
- Abib, A.H., and Jaluria, Y., 1992, "Penetrative Convection in Partial Open Enclosure", to appear in *ASME-AIChE Nat. Heat Transfer Conference*, San Diego, CA.
- Cheesewright, R., King, K.J., and Ziai, S., 1986, "Experimental Data for the Validation of Computer Codes for the Prediction of Two-Dimensional Buoyant Cavity Flows", *In Significant Questions in Buoyancy Affected Enclosure or Cavity Flows*,

- Vol. HTD-60, pp. 75-81, ASME, New York, NY.
- Chen, C.F., Briggs, D.B. and Wirtz, R.A., 1971, "Stability of Thermal Convection in a Salinity Gradient Due to Lateral Heating", *Int. J. Heat Mass Transfer*, Vol. 14, pp. 57.
- Cooper, L.Y., Harkleroad, M., Quintiere, J.G., and Rinkinen, R., 1982, "An Experimental Study of Upper Hot Layer Stratification in Full-Scale Multiroom Fire Scenario", *J. Heat Transfer*, Vol. 104, pp. 741.
- Davidson, L., 1990, "Calculation of the Turbulent Buoyancy-driven Flow in a Rectangular Cavity Using an Efficient Solver and Two Different Low Reynolds  $k-\epsilon$  Turbulence Models", *Numerical Heat Transfer*, Part A, Vol. 18, pp. 129-147.
- Emmons, H.W., 1978, "The Prediction of Fire in Buildings", *17th Symp. (int.) Combustion*, Combustion Institute, pp. 1101.
- Fraikin, M.P., Portier, J.J., and Fraikin, C.J., 1980, "Application of a  $k-\epsilon$  Turbulence Model to an Enclosed Buoyancy Driven Recirculating Flow", *ASME-AIChE Nat. Heat Transfer Conference*, Paper No. 80-HT-68.
- Fusegi, T., and Farouk, B., 1989, "Laminar and Turbulent Natural Convection-Radiation Interaction in a Square Enclosure Filled with a Nongray Gas", *Numer. Heat Transfer*, Part A, Vol. 15, pp. 303-322.
- Gill, A.E., 1966, "The Boundary Layer Regime for Convection in a rectangular cavity", *J. Fluid Mech.*, Vol. 26, pp. 515-536.
- Henkes, R.A.W.M., 1990, "Natural Convection Boundary Layers", *Ph.D. Thesis*, Delft University, Delft, The Netherlands.
- Jaluria, Y., 1980, "Natural Convection Heat and Mass Transfer", Pergamon Press, U.K.
- Jones, W.P., and Launder, B.E., 1972, "The prediction of Laminarization with a Two-Equation Model of Turbulence", *Int. J. Heat Mass Transfer*, Vol. 15, pp. 301-314.
- Kapoor, K., and Jaluria, Y., 1988, "An Experimental Study of the Generation and Characteristics of a Two-Layer Thermally Stable Environment", *Int. Comm. Heat Mass Transfer*, Vol. 15, pp. 751-764.
- Kawagoe, K., 1958, "Fire Behavior in Rooms", *Rep. 27*, Building Research Institute, Japan.
- Ku, A.C., Doria, M.L., Lloyd, J. R., 1976, "Numerical Modeling of Buoyant Flows Generated by Fire in a Corridor", *Proc. 16th Symp. (int.) on Combustion*, Combustion Institute, pp. 1372-1384.
- Larson, D.W., and Viskanta, R., 1976, "Transient Combined Laminar Free Convection and Radiation in a Rectangular Enclosure", *Journal of Fluid Mechanics*, Vol. 78, pp. 65-85.
- Launder, B.E., and Spalding, D.B., 1974, "The Numerical Computation of Turbulent Flows", *Comput. Meth. Appl. Mech. Eng.*, Vol. 3, pp. 269-289.
- List, E.J., 1982, "Turbulent Jets and Plumes", *Ann. Rev. Fluid Mech.*, Vol. 14, pp. 189-212.
- Markatos, N.C., Malin, M.R., and Cox, G., 1982, "Mathematical Modeling of Buoyancy-Induced Smoke Flow in Enclosures", *Int. J. Heat Mass Transfer*, Vol. 25, pp. 63-75.
- Markatos, N.C., and Pericleous, K.A., 1983, "An Investigation of Three-dimensional Fires in Enclosures", in Quintiere, J.G., et al. (Eds.), *Fire Dynamics and Heat Transfer*, HTD-Vol. 25, ASME, New York, NY, pp. 115-124.
- McCaffrey, B.J., and Quintiere, J.G., 1977, "Buoyancy Driven Countercurrent Flow Generated by a Fire Source", in Spalding, D.B., and Afgan, N. (Eds.), *Heat Transfer and Turbulent Buoyant Convection*, Vol. II, pp. 457-472, Hemisphere, Publishing Corp., New York.
- Patankar, S.V., 1980, "Numerical Heat Transfer and Fluid Flow", Hemisphere Publishing Corp., New York.
- Patterson, J. and Imberger, J., 1980, "Unsteady Natural Convection in a Rectangular Cavity", *J. Fluid Mech.*, Vol. 100, pp. 65-86.
- Quintiere, J.G., 1977, "Growth of Fire in Building Compartments", in Robertson, A.F., (Ed.), *Fire Standards and Safety*, ASTM STP 614, American Soc. for Testing and Materials, pp. 131-167.
- Quintiere, J.G., 1984, "Perspective on Compartment Fire Growth", *Combust. Sci. Technol.*, Vol. 39, pp. 11-54.
- Roache, P.J., 1972, "Computational Fluid Dynamics", Hermosa Publishers, Albuquerque, New Mexico.
- Rodi, W., 1980, "Turbulence Models and Their Application in Hydraulics, a State of the Art Review", *International Association for Hydraulics Research*, Delft, The Netherlands.
- Rodi, W., 1987, "Examples of Calculation Methods for Flow and Mixing in Stratified Fluids", *J. Geophys. Res.*, Vol. 92, No. C5, pp. 5305-5328.
- Satoh, K., Yang, K.T., and Lloyd, J. R., 1980, "Ventilation and Smoke Layer Thickness Through a Doorway of a Cubic Enclosure with Central Volumetric Heat Source", *Proc. 1980 Fall Meeting of the Eastern Section of the Combustion Institute*, Paper No. 25.
- Simcox, S., Wilkes, N.S., and Jones, I.P., 1989, "Computer Simulation of the Flow of Hot Gases from the Fire at King's Cross Underground Station", *Proc. Symp. King's Cross Underground Fire*, pp. 19-25, London: Inst. Mech. Eng.
- Thompson, C.P., Wilkes, N.S. and Jones, I.P., 1987, "Numerical Studies of Buoyancy-Driven Turbulent Flow in a Rectangular Cavity", *Int. J. Num. Meth. Engng.*, Vol. 24, pp. 89-99.
- Torrance, K.E., 1979, "Natural Convection in Thermally Stratified Enclosures with Localized Heating from Below", *J. Fluid Mech.*, Vol. 95, pp. 477-495.
- Turner, J.S., 1973, "Buoyancy Effects in Fluids", Cambridge University press, London.
- Walsh, G., 1971, "Contained Non-homogeneous flow under Gravity or How to Stratify a Fluid in the Laboratory", *J. Fluid Mech.*, Vol. 48, pp. 647.
- Yang, K.T., and Lloyd, J.R., 1985, "Natural Convection-Radiation Interaction in Enclosures", *Natural Convection: Fundamentals and Applications*, ed. Aung, W., Kakac, S., and Viskanta, R., Hemisphere Publishing Corp., New York.